

## Experimentally and Computationally Fast Method for Estimation of the Mean Kurtosis

Brian Hansen<sup>1</sup>, Torben E. Lund<sup>1</sup>, Ryan Sangill<sup>1</sup>, and Sune N. Jespersen<sup>1,2</sup>

<sup>1</sup>CFIN, Aarhus University, Aarhus C, Denmark, <sup>2</sup>Department of Physics, Aarhus University, Aarhus C, Denmark

**Introduction:** Diffusion kurtosis imaging (DKI) is a popular extension of diffusion tensor imaging (DTI) accounting for nongaussian aspects of diffusion in biological tissue<sup>1</sup>. Recently, several studies have indicated enhanced sensitivity of mean kurtosis (MK) to tissue pathology, including stroke<sup>2-4</sup>. However, the relatively lengthy acquisition time and postprocessing required to estimate kurtosis metrics remains a barrier for further investigations, and hence current research efforts are directed at speeding up DKI<sup>5</sup>. Here we propose a very fast acquisition and postprocessing scheme for estimation of a new mean kurtosis, which is demonstrated on a large diffusion MR data set from fixed rat brain and a large data set from in-vivo human brain to be very similar to MK. We then introduce and evaluate a fast experimental protocol for estimation of this new mean kurtosis. This protocol requires only 13 diffusion weighted images, which can be acquired in less than one minute, followed by a postprocessing time of seconds. Thus, our new measure is shown to be a clinically feasible alternative to MK, even in an acute setting.

**Theory:** The mean kurtosis is tedious to estimate because it is the orientational average of the apparent kurtosis  $K(\hat{n})$  in the direction  $\hat{n}$ , which is multiplied by the apparent diffusivity  $D(\hat{n})$  in the cumulant expansion of the signal

$$\log S(b, \hat{n}) = -bD(\hat{n}) + \frac{b^2}{6} D(\hat{n})^2 K(\hat{n}) + O(b^4) = -bD(\hat{n}) + \frac{b^2}{6} \bar{D}^2 W(\hat{n}) + O(b^4) \quad (1)$$

Therefore, it is necessary to decouple  $D(\hat{n})$  and  $K(\hat{n})$  before averaging over directions. Here,  $W(\hat{n})$  is related to the kurtosis tensor<sup>1</sup>  $W_{ijkl}$  as  $W(\hat{n}) = \sum_{ijkl} W_{ijkl} n_i n_j n_k n_l$ . To circumvent this difficulty, we propose instead to consider,  $\bar{W}$  the orientationally averaged value of  $W(\hat{n})$

$$\bar{W} = \frac{1}{4\pi} \int d\hat{n} W(\hat{n}) = \frac{1}{4\pi} \sum_{ijkl} W_{ijkl} \int d\hat{n} n_i n_j n_k n_l = \frac{1}{5} (W_{xxxx} + W_{yyyy} + W_{zzzz} + 2W_{xyxy} + 2W_{xzyz} + 2W_{yxzy}) = \frac{1}{5} \text{Tr}(W) \quad (2)$$

Because of Eq. (1), linear combinations of  $W(\hat{n})$  along different directions as in Eq. (2) can be directly estimated by combining log of signals with diffusion gradients along corresponding directions. For example, we find that with 9 directions

$$\frac{1}{15} \left( \sum_{i=1}^3 \log S(b, \hat{n}^{(i)}) + 2 \sum_{i=1}^3 \log S(b, \hat{n}^{(i+)}) + 2 \sum_{i=1}^3 \log S(b, \hat{n}^{(i-)}) \right) = -b\bar{D} + 1/6 b^2 \bar{D}^2 \bar{W} \quad (3)$$

where  $\hat{n}^{(i)}$ ,  $\hat{n}^{(i+)}$  and  $\hat{n}^{(i-)}$  ( $i=1,2,3$ ), are defined as  $\hat{n}^{(1)} = (1,0,0)^T$ ,  $\hat{n}^{(1+)} = (0,1,1)^T$ ,  $\hat{n}^{(1-)} = (0,1,-1)^T$ , and similarly for  $i=2$  and  $3$ ; i.e., superscript  $i$  in  $\hat{n}^{(i+)}$  and  $\hat{n}^{(i-)}$  labels the position of the '0'. Finally, in order to extract  $\bar{W}$ , we need to obtain an estimate of  $\bar{D}$ . We do so by acquiring an additional 3 images along  $\hat{n}^{(i)}$  at a lower b-value, and using the procedure in<sup>5</sup> to estimate the apparent diffusivity along these 3 directions, followed by averaging to obtain  $\bar{D}$ . We will refer to this protocol as the 1-3-9 protocol, and the associated estimate of  $\bar{W}$  as  $\bar{W}_{139}$ .

**Methods:** Fixed rat brain was imaged<sup>6</sup> at 16.4T (Bruker Biospin) using a standard spin echo diffusion weighted sequence. Nine b=0 images were acquired and 144 diffusion weighting directions were chosen to constitute a 144 point spherical 16-design<sup>7</sup> and distributed equally on 16 shells from b=1...15 ms/ $\mu\text{m}^2$ . The remaining diffusion and imaging parameters were: TR=3 s, TE=14.7 ms, data matrix 128x128, field of view 12.8 mmx12.8 mm, slice thickness 0.5 mm, and  $\Delta/\delta=8/2$  ms. Imaging in a human volunteer was performed on a Siemens Trio using a 32 channel head coil. For comparison to the  $\bar{W}$ , we obtained two 160 image data sets for estimation of the full kurtosis tensor and MK in a traditional way. These data sets were recorded using the optimized DKI protocol from<sup>8</sup> with 10 b=0 images and 30 encoding directions on 5 shells at 500, 1000, 1500, 2000, and 2500 s/mm<sup>2</sup>. The fast 1-3-9 protocol was based on the same sequence but used instead one b=0 image, 3 low b-value measurements at b = 1000 s/mm<sup>2</sup>, and 9 directions at b=2500 s/mm<sup>2</sup>. In both data set types, we obtained full brain coverage at 3 mm isotropic resolution. Acquisition time for the fast protocol was 55 secs, followed by smoothing (linear interpolation) and a 2 sec (Matlab® on standard PC) postprocessing procedure as described above. This is to be compared to 11.5 min acquisition time for the 160 image data set, with an associated postprocessing time of about 4 hours in our implementation.

**Results:** To compare the similarity of information in MK and  $\bar{W}$ , Fig. 1 shows maps of both metrics as computed explicitly from the full kurtosis tensor determined from a fit of the rat data to Eq. (1). The contrast is highly comparable but the arrow indicates a region where the two maps differ appreciably. A scatter plot of the two maps against each other

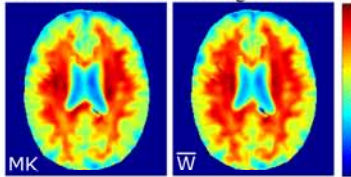


**Fig.2:** Comparison of MK and  $\bar{W}$  in normal human brain.

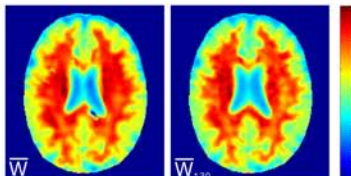


**Fig. 3:** Comparison of  $\bar{W}$  from full kurtosis tensor and  $\bar{W}_{139}$  obtained using the fast protocol.

over the 8 repetitions of the 139 protocol, showing that it is less than 10% over most parts of the brain.

**Conclusions:** We have suggested a new kurtosis metric  $\bar{W}$ , which can be defined as the isotropic part of the kurtosis tensor. We showed experimentally that  $\bar{W}$  maps had very similar contrast to the conventional mean kurtosis, MK. Therefore, we expect  $\bar{W}$  to share many of the same characteristics as MK, in particular it gives reason to believe that  $\bar{W}$  could be a valuable marker of tissue pathology. In contrast to MK, however,  $\bar{W}$  is extremely fast to measure, and the scheme proposed here would enable  $\bar{W}$  to be estimated in practically any clinical setting with negligible acquisition time overhead and a post-processing time of a few seconds. We believe our method will facilitate a more rapid exploration of the potential applications of DKI.

**References:** 1. Jensen, J.H., et al., Magn. Reson. Med., (2005). 53;2. Hui, E.S., et al., Stroke, (2012);3. Jensen, J.H., et al., NMR Biomed, (2011). 24;4. Latt, J., et al. in Proc. Int. Soc. Magn. Reson. Med. 2009;5. Jensen, J.H., et al. in Proc. Int. Soc. Magn. Reson. Med. 2009. Honolulu, Hawaii.; 6. Jespersen, S.N., et al., Neuroimage, (2010). 49;7. Hardin, R.H. and N.J.A. Sloane, Discrete & Computational Geometry, (1996). 15;8. Poot, D.H., et al., IEEE Trans Med Imaging, (2010). 29;

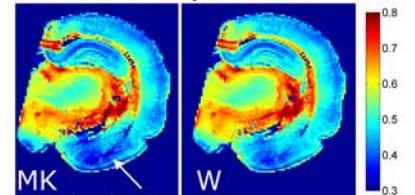


**Fig. 1:** MK and  $\bar{W}$  in a fixed rat brain.

has a linear correlation of 0.88, and in fact, more than 90% of the MK values are within 10% of the  $\bar{W}$  value in the same pixel. The similarity between MK and  $\bar{W}$  is also seen in the human data: Fig. 2 shows MK and  $\bar{W}$  estimated from a fit to a 160 image DKI data set. Again the contrast is comparable, and a scatter plot of the human data in Fig. 2 revealed a linear correlation of 0.99 with 96% of the MK values within 10% of corresponding  $\bar{W}$  value. Having thus established the similarity of MK and  $\bar{W}$  we now turn to comparing  $\bar{W}$  as obtained from a 160 image data set to  $\bar{W}_{139}$ .

Figure 3 shows maps of  $\bar{W}$  and  $\bar{W}_{139}$  and it is seen that the contrast in  $\bar{W}_{139}$  from the fast protocol is clearly of a similar nature to that from the full data set, however, differences are visible. Most notably,  $\bar{W}_{139}$  values from the fast protocol seem to underestimate the extent of regions with higher values of  $\bar{W}$ . Comparing the  $\bar{W}$  maps obtained from two 160 image data sets to eight  $\bar{W}_{139}$  maps obtained from 8 acquisitions of the 1-3-9 data sets, we

find an average linear correlation of 0.97, and an average of 87% of the  $\bar{W}$  values from the full data sets were estimated with a 10% accuracy by  $\bar{W}_{139}$ . Lastly, we consider in Fig. 4 the robustness of the fast protocol, by comparing the percentage difference between 2 repetitions (A) to a similar measure for mean kurtosis (B) using the full data set for the latter. Most of the voxels change less than 10%, and the robustness of  $\bar{W}_{139}$  is seen to be comparable to MK, despite being based on a much smaller data set. Figure 4C examines the coefficient of variation

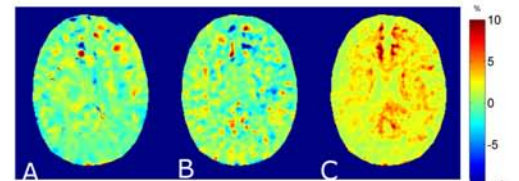


**Fig.4:** Robustness of  $\bar{W}$  and  $\bar{W}_{139}$ .